

On the crack propagation modeling of hydraulic fracturing by a hybridized displacement discontinuity/boundary collocation method

M. Behnia¹, K. Goshtasbi^{2*}, M. Fatehi Marji³, A. Golshani⁴

1,2. Department of mining Engineering, Faculty of Eng., Tarbiat Modares University, Tehran, Iran

3. Faculty of Mining Engineering, Yazd University, Yazd, Iran

4. Department of Civil Engineering, Faculty of Eng., Tarbiat Modares University, Tehran, Iran

Received 15 Mar 2011; received in revised form 1 Jul 2011; accepted 30 Oct 2011

*Corresponding author: goshtasb@modares.ac.ir

Abstract

Numerical methods such as boundary element and finite element methods are widely used for the stress analysis in solid mechanics. This study presents boundary element method based on the displacement discontinuity formulation to solve general problems of interaction between hydraulic fracturing and discontinuities. The crack tip element and a higher order boundary displacement collocation technique are used to study the hydraulic fracture propagation and its interaction with the pre-existing cracks and discontinuities in an elastic rock mass. The maximum tangential stress criterion (or σ -criterion) and the strain energy density criterion (SED) are used to obtain the fracture path and the results of both criteria are compared with each other. The comparison of numerical method with the results brought in the literature shows a good performance of the method in the case of interacting cracks.

Keywords: *Hydraulic fracturing; displacement discontinuity method; displacement collocation technique; rock fracture mechanics; crack interaction; fracture propagation criteria.*

1. Introduction

Hydraulic fracturing has been used in the petroleum industry as a stimulation technique to enhance oil and gas recovery in low permeability reservoirs and for estimating in situ stresses [1].

One of the important features needed in fracture design is the ability to predict the geometry and the characteristics of hydraulically induced fracture.

Because of the presence of discontinuities in the rock mass, a better understanding of how an induced fracture interacts with a discontinuity is fundamental for predicting the ultimate size and shape of the hydraulic fractures formed by a treatment. Theoretical and experimental investigations of fracture initiation, propagation, and interaction with pre-existing geological discontinuities based on fracture mechanics theory

began during the 1960s and work continues on this topic.

In general, three approaches can be used to analyze the mechanics of crack problems: (1) Continuum damage mechanics [2,3]; (2) stochastic damage mechanics [4]; and (3) Fracture mechanics simulation using numerical methods such as boundary element methods [5,6,7].

Boundary element method (BEM) is one of the powerful numerical methods and has been extensively used in fracture mechanics [8,9]. In terms of computational resources, BEM is more efficient than other methods, including FEM, for crack problems where surface/volume ratio is small and stress changes rapidly. The database for a boundary element method analysis is much smaller than that of a finite element method analysis because only the boundaries of the

structure, including the crack faces, need to be discretized. Displacement discontinuity method (DDM) is an indirect boundary element method, which has been used for the analysis of crack problems related to rock fracture mechanics. It should be noted that DDM does not have the re-meshing problem. Examples can be found in Olson and Pollard (1988, 1989, and 1991), Chan et al. (1990), Pollard et al. (1990), Zeller and Pollard (1992), Shen and Stephansson (1994), Scavia (1995), Marji M. F. (1997), among many others [10-15, 5, 16, and 17].

Recently the higher order variations of the displacement discontinuities with special crack tip elements are usually used for the treatment of crack problems [16, 18-22].

Some numerical codes simulate the effect of pre-existing fractures explicitly, and some of them are designed to model the fracture initiation and propagation of individual cracks with DDM. FROCK is a two-dimensional Hybridized Indirect Boundary Element Method that uses the constant and linear element to model the brittle behavior of materials with multiple flaws in a finite or infinite medium [13,23]. The recent fracture codes like FRACOD (The two-dimensional boundary element code with constant element) based on F-criterion has been used to model the fracture propagation and interaction of randomly distributed fractures in rock [5, 24].

Dong and de Pater (2001) investigated the effect of fault on crack reorientation by DDM [7]. They used the higher order element and crack tip element with maximum tangential stress criterion to model the hydraulic fracture propagation near the interface.

Based on linear elastic fracture mechanics, three fundamental fracture criteria, i.e, the maximum tangential stress criterion (MTS or σ -criterion) [25], the maximum strain energy release rate criterion (or G-criterion) [26], and the minimum strain energy density criterion (SED or S-criterion) [27] have been mostly used to study the fracture behavior of brittle materials [28,29,30]. All of these criteria have demonstrated that a crack in a plate under a general in-plane load does not initiate and propagate in its original plane, but rather crack initiation takes place at an angle with respect to the crack plane.

Among these three fracture criteria, the S-criterion is the most difficult to understand and to use. It is based on the minimum strain energy density

concept. When the minimum strain energy density attains a critical value of the material, the crack initiation takes place. S-criterion considers the complete energy field both local and global, which varies from point to point in materials. Using this criterion the location of crack initiation, the crack path, and the point of final termination can be determined. Experimental results on Indiana limestone and Westerly granite [31] showed that the S-criterion is the most accurate of the three theories used for comparison.

In the present work, for estimation of the crack path direction, the S-criterion is implemented numerically to handle the fracture propagation mechanism in rock type material considering the finite and infinite bodies and it is used to study interaction of the pressurized fracture with discontinuities. The results are compared with the results of mixed mode σ -criterion. A general higher order displacement discontinuity method (quadratic element) implementing crack tip element for each crack end is used to show how the crack tip interaction affects on the behavior, geometry of the fractures, crack opening displacement (COD) and stress intensity factors (SIF).

All simulations are two-dimensional, plane strain, and assume linear-elastic, homogenous materials. Some example problems are solved and the computed results are compared with the results given in the literature.

2. Higher Order Displacement Discontinuity Method

A displacement discontinuity element with length of $2a$ along the x-axis is shown in figure 1 (a), which is characterized by a general displacement discontinuity distribution of $u(\varepsilon)$. By taking the u_x and u_y components of the general displacement discontinuity $u(\varepsilon)$ to be constant and equal to D_x and D_y respectively, in the interval $(-a, +a)$ as shown in Figure 1 (b), two displacement discontinuity element surfaces can be distinguished, one on the positive side of y ($y=0+$) and another one on the negative side ($y=0-$). The displacements undergo a constant change in value when passing from one side of the displacement discontinuity element to the other side. Therefore, the constant element displacement discontinuities D_x and D_y can be written as:

$$D_x = u_x(x,0_-) - u_x(x,0_+), D_y = u_y(x,0_-) - u_y(x,0_+) \quad (1)$$

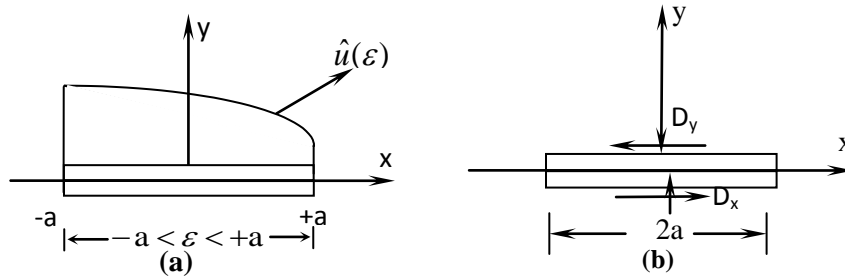


Figure1. (a) Displacement discontinuity element and the distribution of $u(\epsilon)$, (b) Constant element displacement discontinuity

The positive sign convention of D_x and D_y is shown in Figure 1 (b) and demonstrates that when the two surfaces of the displacement discontinuity overlap D_y is positive, which leads to a physically impossible situation. This conceptual difficulty is overcome by considering that the element has a finite thickness, in its undeformed state which is small compared to its length, but larger than D_y [32, 33].

2.1. Quadratic Element Formulation

The quadratic element displacement discontinuity is based on analytical integration of quadratic collocation shape functions over collinear, straight-line displacement discontinuity elements [18]. Figure 2 shows the quadratic displacement discontinuity distribution, which can be written in a general form as

$$D_i(\epsilon) = N_1(\epsilon)D_i^1 + N_2(\epsilon)D_i^2 + N_3(\epsilon)D_i^3 \quad (2)$$

$$i = x, y$$

Where, D_i^1 , D_i^2 , and D_i^3 are the quadratic nodal displacement discontinuities, and

$$\begin{aligned} N_1(\epsilon) &= \epsilon(\epsilon - 2a_1)/8a_1^2 \\ N_2(\epsilon) &= -(\epsilon^2 - 4a_1^2)/4a_1^2 \\ N_3(\epsilon) &= \epsilon(\epsilon + 2a_1)/8a_1^2 \end{aligned} \quad (3)$$

are the quadratic collocation shape functions using $a_1 = a_2 = a_3$. A quadratic element has 3 nodes, which are at the centers of its three sub-elements. The displacements and stresses for a line crack in an infinite body along the x-axis, in terms of single harmonic functions $g(x,y)$ and $f(x,y)$, are given by Crouch and Starfield (1983) [33] as:

$$\begin{aligned} u_x &= [2(1-\nu)f_{,y} - yf_{,xx}] + \\ &[-(1-2\nu)g_{,x} - yg_{,xy}] \\ u_y &= [(1-2\nu)f_{,x} - yf_{,xy}] + \\ &[2(1-\nu)g_{,y} - yg_{,yy}] \end{aligned} \quad (4)$$

and the stresses are:

$$\begin{aligned} \sigma_{xx} &= 2\mu[2f_{,xy} + yf_{,xyy}] + \\ &2\mu[g_{,yy} + yg_{,yyy}] \\ \sigma_{yy} &= 2\mu[-yf_{,xyy}] + \\ &2\mu[g_{,yy} - yg_{,yyy}] \\ \sigma_{xy} &= 2\mu[2f_{,yy} + yf_{,yyy}] + \\ &2\mu[-yg_{,xyy}] \end{aligned} \quad (5)$$

μ is shear modulus and, $f_{,x}$, $g_{,x}$, $f_{,y}$, $g_{,y}$, etc. are the partial derivatives of the single harmonic functions $f(x,y)$ and $g(x,y)$ with respect to x and y , in which these potential functions for the quadratic element case can be found from:

$$f(x, y) = \frac{-1}{4\pi(1-\nu)} \sum_{j=1}^3 D_x^j F_j(I_0, I_1, I_2) \quad (6)$$

$$g(x, y) = \frac{-1}{4\pi(1-\nu)} \sum_{j=1}^3 D_y^j F_j(I_0, I_1, I_2)$$

in which, the common function F_j , is defined as:

$$F_j(I_0, I_1, I_2) = \int N_j(\epsilon) \ln[(x-\epsilon)^2 + y^2]^{\frac{1}{2}} d\epsilon \quad (7)$$

$j = 1, \text{ to } 3$

where, the integrals I_0 , I_1 and I_2 are expressed as follows:

$$I_0(x, y) = \int_{-a}^a \ln[(x-\epsilon)^2 + y^2]^{\frac{1}{2}} d\epsilon = \quad (8-a)$$

$$y(\theta_1 - \theta_2) - (x-a)\ln(r_1) + (x+a)\ln(r_2) - 2a$$

$$I_1(x, y) = \int_{-a}^a \epsilon \ln[(x-\epsilon)^2 + y^2]^{\frac{1}{2}} d\epsilon = \quad (8-b)$$

$$xy(\theta_1 - \theta_2) + 0.5(y^2 - x^2 + a^2)\ln\frac{r_1}{r_2} - ax$$

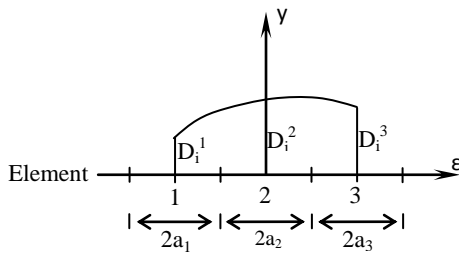


Figure 2. Quadratic collocations for the higher order displacement discontinuity elements

$$\begin{aligned}
 I_2(x, y) &= \int_{-a}^a \varepsilon^2 \ln[(x - \varepsilon)^2 + y^2]^{\frac{1}{2}} d\varepsilon = \\
 &\frac{y}{3}(3x^2 - y^2)(\theta_1 - \theta_2) \\
 &+ \frac{1}{3}(3xy^2 - x^3 + a^3) \ln(r_1) \\
 &- \frac{1}{3}(3xy^2 - x^3 - a^3) \ln(r_2) \\
 &- \frac{2a}{3}(x^2 - y^2 + \frac{a^2}{3})
 \end{aligned} \tag{8-c}$$

The terms θ_1 , θ_2 , r_1 and r_2 in this equation are defined as:

$$\begin{aligned}
 \theta_1 &= \arctan\left(\frac{y}{x-a}\right), & \theta_2 &= \arctan\left(\frac{y}{x+a}\right), \\
 r_1 &= [(x-a)^2 + y^2]^{\frac{1}{2}}, & \text{and } r_2 &= [(x+a)^2 + y^2]^{\frac{1}{2}}
 \end{aligned}$$

3. Stress Intensity Factor and Crack Tip Element

The stress intensity factor is an important concept in fracture mechanics. Considering a body of arbitrary shape with a crack of arbitrary size, subjected to arbitrary tensile and shear loadings (i.e. the mixed mode loading I and II), the stresses and displacements near the crack tip are given in general text books [30, 34], but as we use the displacement discontinuity method here we need

the formulations given for the SIF (K_I and K_{II}) in terms of the normal and shear displacement discontinuities [18, 30].

Based on LEFM theory, the Mode I and Mode II stress intensity factors K_I and K_{II} can be written in terms of the normal and shear displacement discontinuities as [18]:

$$\begin{aligned}
 K_I &= \frac{\mu}{4(1-\nu)} \left(\frac{2\pi}{a}\right)^{\frac{1}{2}} D_y(a), \\
 K_{II} &= \frac{\mu}{4(1-\nu)} \left(\frac{2\pi}{a}\right)^{\frac{1}{2}} D_x(a)
 \end{aligned} \tag{9}$$

Analytical solutions to crack problems for various loading conditions show that the stresses at the distance r from the crack tip always vary as $r^{-0.5}$ if r is small. Due to the singularity variations $1/\sqrt{r}$ and \sqrt{r} for the stresses and displacements at the vicinity of the crack tip the accuracy of the displacement discontinuity method decreases, and usually a special treatment of the crack at the tip is necessary to increase the accuracy and make the method more efficient. A special crack tip element which already has been introduced in literature (e.g. [18]) is used here, to represent the singularity feature of the crack tip. Using the special crack tip element of length $2a$, as shown in figure 3, the parabolic displacement discontinuity variations along this element are given as:

$$D_i(\varepsilon) = D_i(a) \left(\varepsilon/a\right)^{\frac{1}{2}}, \quad i = x, y \tag{10}$$

Where, ε is the distance from crack tip and $D_y(a)$ and $D_x(a)$ are the opening (normal) and sliding (shear) displacement discontinuities at the center of special crack tip element.

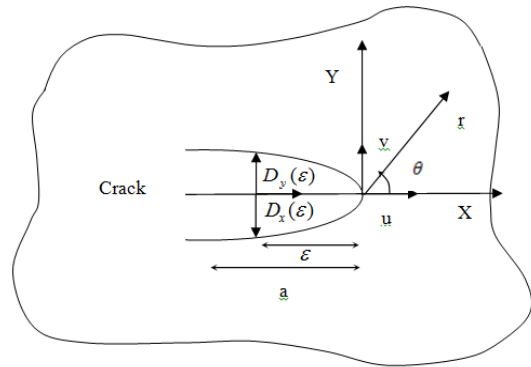


Figure 3. Displacement correlation technique for the special crack tip element

Substituting equation (10) into equations (4) and (5), the displacement and stresses can be expressed in terms of $D_i(a)$.

The potential functions $f_C(x, y)$ and $g_C(x, y)$ for the crack tip element can be expressed as:

$$\begin{aligned}
 f_C(x, y) &= \frac{-1}{4\pi(1-\nu)} \int_{-a}^a \frac{D_x(a)}{a^{\frac{1}{2}}} \varepsilon^{\frac{1}{2}} \ln[(x - \varepsilon)^2 + y^2]^{\frac{1}{2}} d\varepsilon \\
 g_C(x, y) &= \frac{-1}{4\pi(1-\nu)} \int_{-a}^a \frac{D_y(a)}{a^{\frac{1}{2}}} \varepsilon^{\frac{1}{2}} \ln[(x - \varepsilon)^2 + y^2]^{\frac{1}{2}} d\varepsilon
 \end{aligned} \tag{11}$$

These functions have a common integral of the following form:

$$I_C = \int_0^{2a} \varepsilon^{\frac{1}{2}} \ln \left[(x - \varepsilon)^2 + y^2 \right]^{\frac{1}{2}} d\varepsilon \quad (12)$$

4. Fracture propagation criterion

In LEFM conditions, crack propagation modeling requires knowledge of two types of parameters: the stress intensity factors, determined analytically and a function of geometry, load, and the appropriate fracture toughness, a material state property, determined experimentally [35].

The mixed mode of stress intensity factors (i.e. Mode I and Mode II fractures, which are the most commonly fracture modes occur in rock fracture mechanics) are numerically computed. Several mixed mode fracture criteria have been used in literature to investigate the crack initiation direction and its path [5, 30, and 36]. As most of rocks have brittle behavior under tension, the mode I fracture toughness K_{IC} (under plain strain condition) with the maximum tangential stress fracture criterion (σ -criterion) introduced by Erdogan and Sih mostly are used to predict the crack propagation direction [25].

This is a widely used mixed mode fracture mechanics criterion and well fitted with some experimental results [28, 37, 38, and 30].

Based on this criterion, the crack tip will start to propagate when:

$$\cos \frac{\theta_0}{2} \left[K_I \cos^2 \frac{\theta_0}{2} - \frac{3}{2} K_{II} \sin \frac{\theta_0}{2} \right] = K_{IC} \quad (13)$$

Where θ_0 is the crack propagation angle follows that:

$$\theta_0 = 2 \arctan \left[\frac{1}{4} \left(\frac{K_I}{K_{II}} \right) - \frac{1}{4} \sqrt{\left(\frac{K_I}{K_{II}} \right)^2 + 8} \right] \quad (14)$$

The latter value corresponding to the crack tip should satisfy the condition:

$$K_I \sin \theta_0 + K_{II} (3 \cos \theta_0 - 1) = 0 \quad (15)$$

Another criterion is the minimum strain energy density (the S-criterion) formulated by Sih(1974) that the parameter which governs cracking is the strain energy density near the crack tip [27]. Crack extension occurs in the direction along which dU/dV(strain energy) possesses a minimum

value, θ_0 such that,

$$\frac{\partial S}{\partial \theta} = 0, \quad \frac{\partial^2 S}{\partial \theta^2} \geq 0 \quad (16)$$

where

$$S = a_{11} K_I^2 + 2a_{12} K_I K_{II} + a_{22} K_{II}^2$$

$$a_{11} = \frac{1}{16\pi G} (1 + \cos \theta) (K - \cos \theta)$$

$$a_{12} = \frac{\sin \theta}{16\pi G} [2 \cos \theta - (K - 1)]$$

$$a_{22} = \frac{1}{16\pi G} [(K + 1)(1 - \cos \theta) + (1 + \cos \theta)(3 \cos \theta - 1)]$$

and the crack extension occurs when $S(\theta_0)$ reaches a critical value, S_C . $S(\theta)$ is evaluated

along a contour $r = r_0$ where r_0 is a material constant. A fracture initiation locus in the $K_I K_{II}$ plane is obtained from

$$1 = \frac{8G}{(K - 1)} \left[a_{11} \left(\frac{K_I}{K_{IC}} \right)^2 + 2a_{12} \frac{K_I K_{II}}{K_{IC}} + a_{22} \left(\frac{K_{II}}{K_{IC}} \right)^2 \right] \quad (17)$$

Experimental results on Indiana limestone and Westerly granite showed that the S-criterion is the most accurate of the three theories used for comparison (figure 4) [31]. Therefore, we used the S-criterion to model the fracture propagation of hydraulic fractures near the discontinuities and then compared the results with σ - criterion.

A fracture propagation model completes when, the fracture increment length of a crack can be predicted. This can be done in two ways: (i) by predicting fracture increment length for a given loading condition and (ii) by predicting the load change required to extend a crack for a given length [35].

For a given crack length of 2b, under a certain loading condition, the crack propagation angle

θ_0 is predicted (based on LEFM principles and σ -Criterion i.e. equations (13) and (14) or S-criterion i.e. equation (16)).

Then the original crack is extended by an amount Δb that has equal length with crack tip element.

This element will be perpendicular to the maximum tangential stress near the crack tip for

σ -criterion or will be perpendicular to the minimum strain energy density in the point ahead

of the crack tip. So a new crack length ($b + \Delta b$) is obtained and again the equations (13) and (14)

for σ -criterion or equation (16) for S-criterion are used to predict the new conditions of crack

propagation for this new crack. This procedure is repeated until the crack stops its propagation or

the material breaks away. This procedure can give a propagation path for a given crack under a certain loading condition.

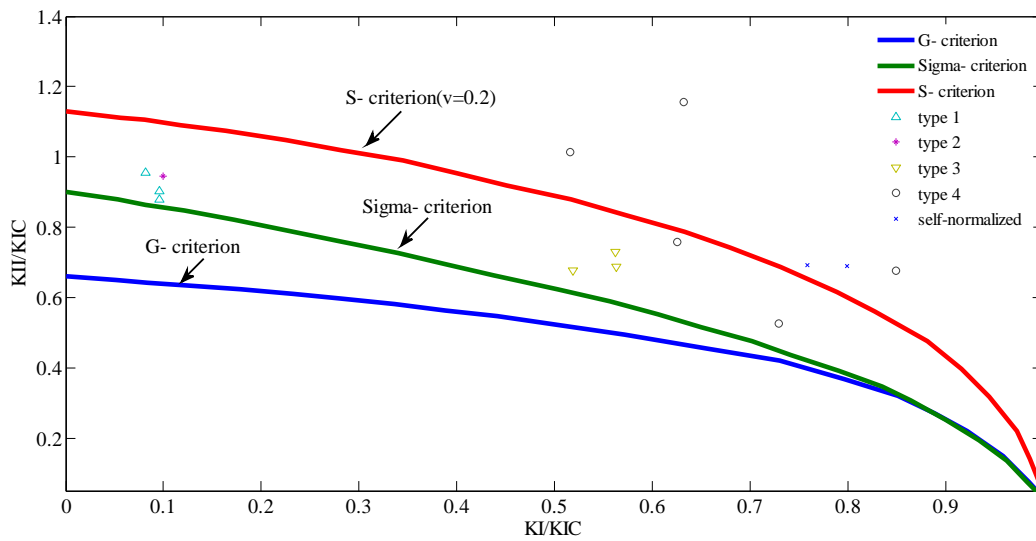


Figure 4. Results from mixed-mode fracture initiation tests for Indiana limestone. From Ingraffea (1981)

5. Verification of higher order displacement discontinuity

Verification of this method (TDDQCR) was made through the solution of several example problems i.e. a pressurized crack in an infinite body, an inclined crack in an infinite body and a circular arc crack under biaxial tension in infinite bodies [20]. In this study, the verification is continued by the two equal cracks under tension in infinite medium, two cracks emanating from Circular hole, and Oriented pressurized crack under compressive far field stresses. These examples are used here because they have analytical solutions or have been solved numerically by other researches, so the computed numerical results can be compared and the validity of the programs can be confirmed. Therefore, the accuracy of the method is demonstrated by example problems because the results are in good agreement with the analytical solutions.

5.1. Interaction between two equal cracks

Interaction of two equal cracks in infinite body is investigated (Figure 5). The crack AB is horizontal and perpendicular to the direction of applied tension stress, and crack CD has different inclinations with horizontal axis. Interaction is considered in two categories that the centers of the cracks have 3a and 2a distance from each other (Figure 5). Materials parameters are taken as $E=10000 \text{ MPa}$, $\nu = 0.2$. Applied stress is 10 MPa and half crack length (a) is 1 m.

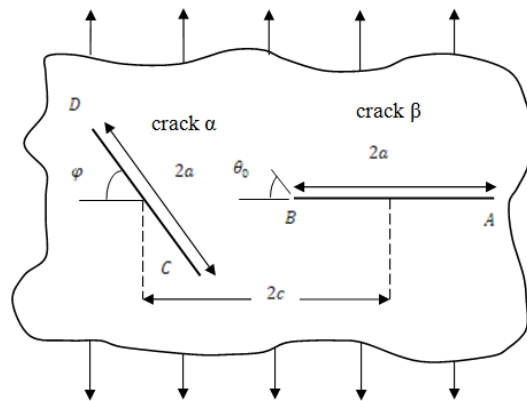


Figure 5. Two equal inclined cracks

With varying the angle φ , the crack propagation angle changes in different distances. The results show when the distance between the centers of two cracks is 3a, the fracture propagation angles have positive values, but in another condition, the fracture propagation angles first have negative angles and then change to positive values (Figure 6). Comparison of the two conditions shows that the decreasing of distance between two cracks causes the influence on the fracture propagation angles. The results from the numerical method with σ -criterion are compared with some results of Gdouts.1984 (Figure 6). Although there are some discrepancies between present results and Gdouts, 1984 [39] (5% error in some angles), the changing trends of the propagation angles are similar to each other.

5.2. Circular hole with two symmetrical cracks

In this study the problem of two equal cracks, emanating from a circular hole in an infinite sheet subjected to a remote tensile stress σ was considered (Figure 7). If a small crack is present, its behavior is governed by the loading and the ratio between the magnitudes of ligament and hole diameter.

In order to show the benefit of both higher order elements and special crack tip elements explained above, this example problem is solved numerically by the higher order displacement discontinuity method using quadratic displacement discontinuity elements.

The following assumptions are made to solve this problem numerically: the far field stress $\sigma = 10$ MPa; the hole radius $R = 0.1$ m; modulus of elasticity $E = 10$ GPa; Poisson's ratio $\nu = 0.2$; and Mode I fracture toughness $K_{Ic} = 2$ MPa m^{1/2} (for a typical hard rock under plane strain condition). The ratio of crack tip element length l to the crack length is 0.25. The comparison between numerical method and the analytical value of the normalized stress intensity factor ($K_I/(\sigma\sqrt{\pi a})$) at different ratio (a/r) obtained from the solutions (Sih, 1973) [40] is presented in the table 1. The numerical results show that general error in most cases is less than about 1%.

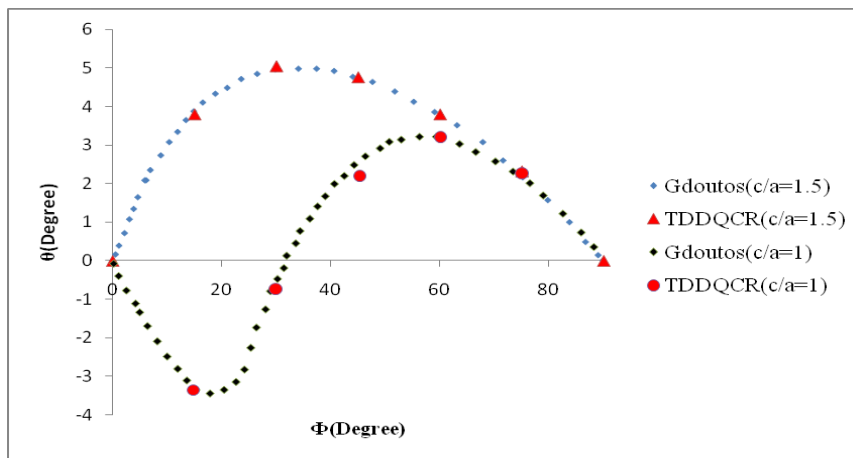


Figure 6. Distribution of fracture propagation angle (θ_{OB}) related to crack inclinations for different distances between centers of cracks

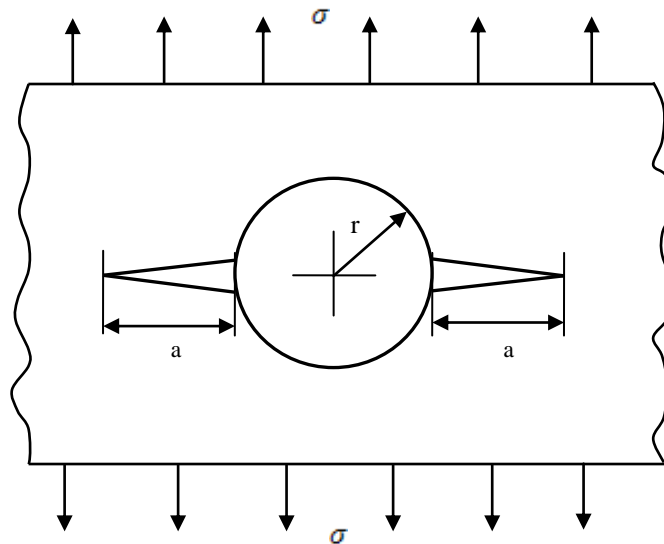


Figure 7. Circular hole with two symmetrical cracks

5.3. Oriented pressurized crack under compressive far field stresses

For verification of numerical method in compressive biaxial loading, the pressurized crack that is oriented at an arbitrarily angle β with respect to the direction of the maximum principal stress, σ_H is studied (Figure 8). For such loaded crack, both the mode I and II stress intensity factors exist at the crack tips, which have been given by (Rice, 1968) [41] as follows:

$$K_I = \sqrt{\pi a} [P - (\sigma_H \sin^2 \beta + \sigma_h \cos^2 \beta)]$$

$$K_{II} = \frac{\sqrt{\pi a}}{2} [\sigma_H - \sigma_h] \sin 2\beta \tag{18}$$

Where a is the half crack length and P is the internal pressure.

The boundary conditions and geometry for numerical solution are the maximum horizontal stress =7 MPa, the minimum horizontal stress =2 MP, pressure inside the fracture $P=10$ MPa, and the half of crack length $a=1$ m. Properties of material are modulus of elasticity $E =10$ GPa, Poisson's ratio $\nu = 0.2$, and Mode I fracture toughness $K_{IC} = 2$ MPa m^{1/2}. The ratio of crack tip element length l to the half of the crack length a is 0.05. Figure 9 shows good agreement between the numerical results and analytical results (the error less than 0.05%) for both of stress intensity factors K_I and K_{II} .

6. Crack reorientation

To show the effect of fluid pressure and horizontal stresses on hydraulic fracturing propagation and reorientation of its path with maximum tangential stress criterion and minimum strain energy density criterion, some problems are solved in relation to pressurized crack in infinite body.

The crack in infinite body with half length of $a=0.02$, and inclination of 90-degree with respect to the X-axis is studied. The physical properties are $E=20$ GPa, $\nu = 0.2$ and the crack toughness of 0.6 MPa m^{0.5}. The maximum and minimum compressive horizontal stresses are 19.4 and 9.7 MPa respectively that σ_H lies in X direction and σ_h is in Y direction.

Figure 10 illustrates the hydraulic fracturing paths for three different pressures inside the crack. The results for both criteria were compared with each other and with Dong, 2001 results. The results show that the S-criterion and σ -criterion are different from each other. These differences are related to the deviate of fracture with large angle and large value of K_{II} near the fracture tip.

It can be found that the low fluid pressure causes the reorientation of fracture to happen sooner; otherwise, the crack tends to propagate in its plane with increasing the fluid pressure. As equation (18) shows, under the same conditions, increasing the fluid pressure increases K_I , but K_{II} is independent of fluid pressure. Then the hydro-fracture tends to propagates in direction near its plane orientation (mode I) by increasing the pressure. These results have good agreement with previous works, i.e. Cornet (1982) [42] that mentioned increasingly large internal pressure will lead to effects of compressive stresses on the crack tip stress field becoming less and less significant so that the fracture reorientation is less marked.

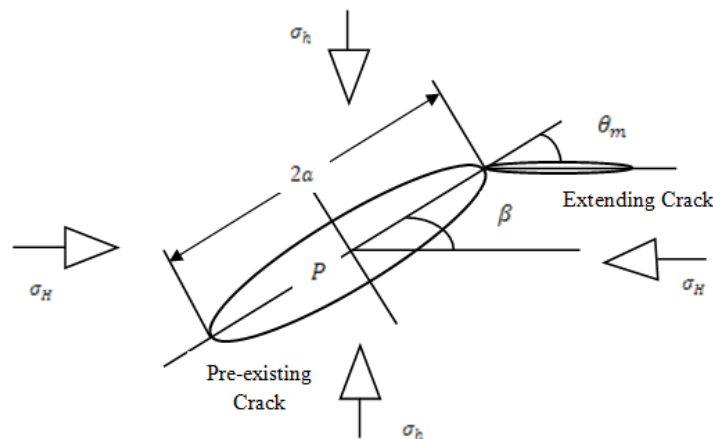


Figure 8. Arbitrarily oriented crack under far field stresses and internal pressure

Table.1. the normalized stress intensity factors $KI/(\sigma\sqrt{\pi a})$ for a hole with two emanating radial cracks at different ratio (a/r)

a/r	$KI/(\sigma\sqrt{\pi a})$ (numerical)	l/b	$KI/(\sigma\sqrt{\pi a})$ (Sih,1973)
0.2	2.36	0.25	2.41
0.4	1.95	0.25	1.96
0.6	1.72	0.25	1.71
0.8	1.58	0.25	1.58
1.0	1.47	0.25	1.45
1.5	1.31	0.25	1.29
2.0	1.22	0.25	1.21

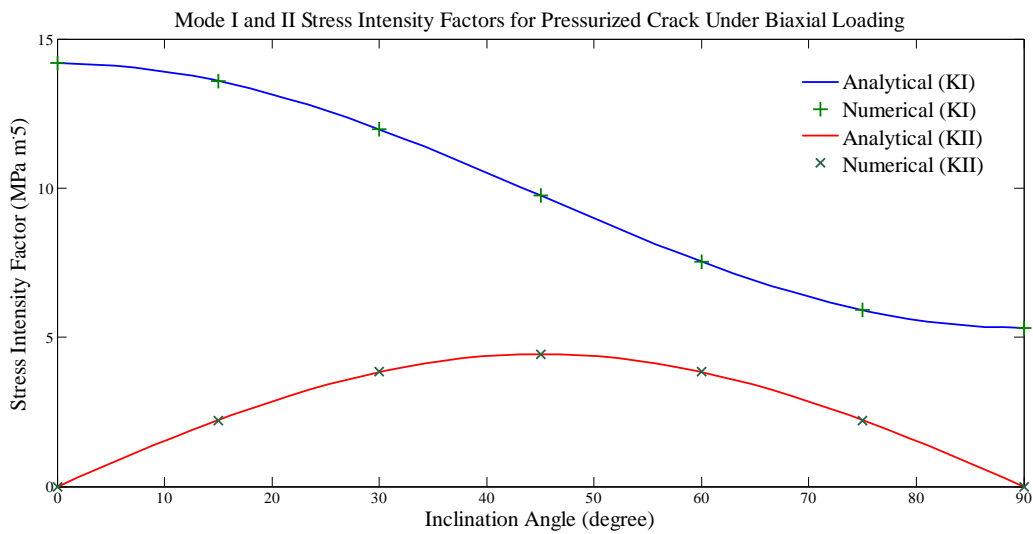


Figure 9. Analytical and numerical values of the stress intensity factors, K_I and K_{II} for the inclined pressurized crack at different orientation from the maximum horizontal stress (X-axis)

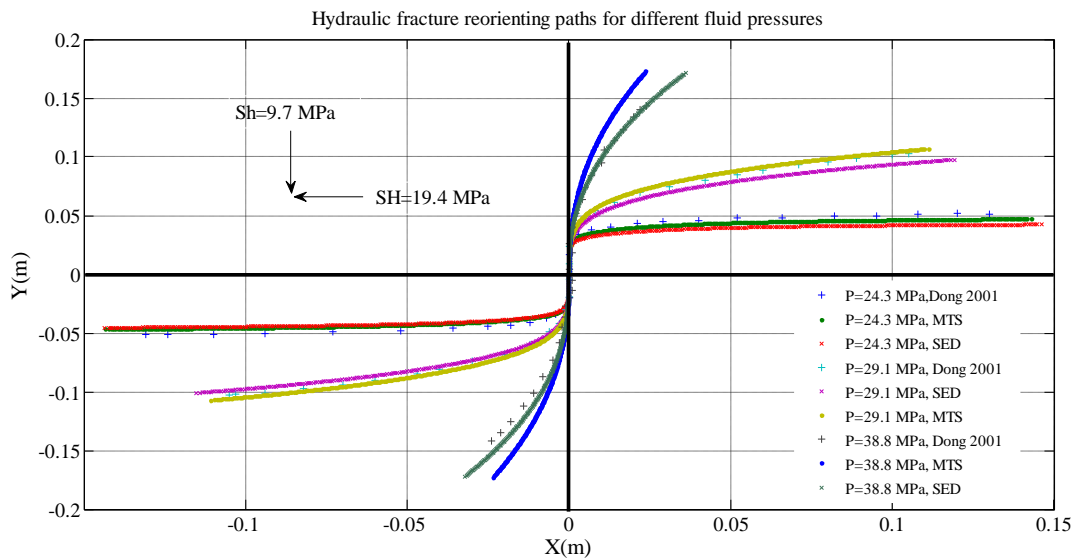


Figure 10. Hydraulic fracture reorientation paths for different fluid pressures. The maximum horizontal stress (X-axis) and minimum horizontal stress (Y-axis) are 19.4 and 9.7 MPa respectively

Figure 11 shows the hydraulic fracture reorientation for three different horizontal stress sets (9.7-9.7, 9.7-19.4, 9.7-22.6 MPa). The maximum horizontal stresses are applied in X-axis, the minimum horizontal stresses are applied in Y-direction, and the pressure inside the crack is

29.1 MPa. The results show that in different compositions of horizontal stresses the paths of hydraulic fracture are different. It can be found that in high horizontal stresses, the fracture reorients sooner, and decreasing horizontal stresses the reorientation occurred later.

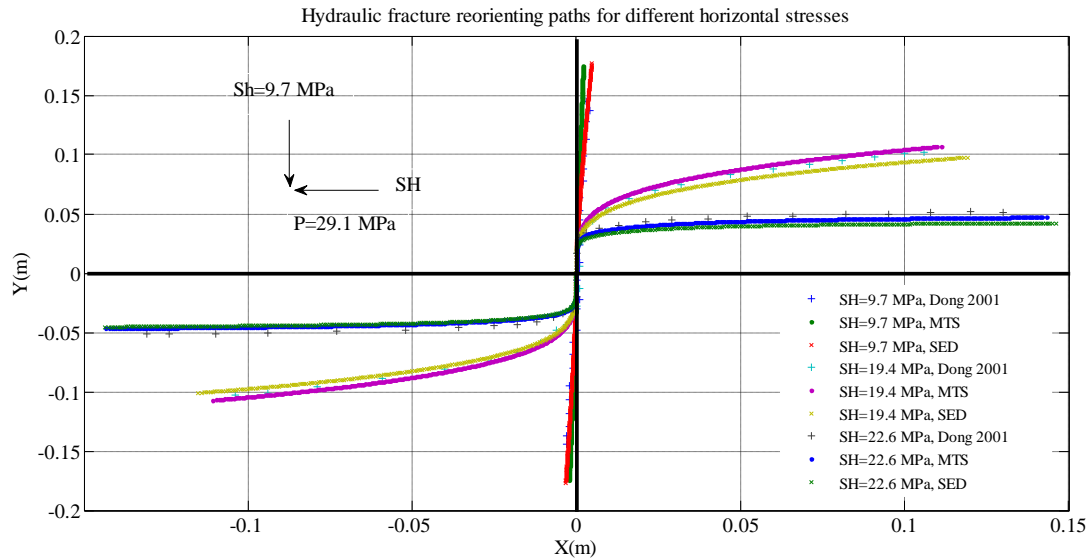


Figure 11. Hydraulic fracture reorientation paths for different horizontal stresses. The fluid pressure inside the fracture is 29.1 MPa

These results from both criteria were compared with Dong, 2001 results. They have agreement with equation (18) too, because by increasing the horizontal stresses, K_{II} will increase and the fracture deviates and tends to propagate in direction far from its plane orientation.

Figure 11 also shows for each stress difference the crack path rotates towards the direction of the maximum horizontal stress. Therefore, the crack tip tends to be under mode I loading and the mode II crack tip stress intensity factor tends to approach zero and the mode I crack tip stress intensity will increase. This result has agreement with previous works (Ching, 1997) [43].

7. Crack interaction

7.1. Crack interaction with discontinuity under far field tensile stresses

For better understanding of how a crack interacts with a discontinuity in body, the field stresses around the crack α , and discontinuity β are studied. The geometry like the example presented in part 5.1 is considered to find the path of fracture propagation and reorientation from the crack to the inclined discontinuity. Figures 12 and 13 show the stress distribution of stress (average of σ_1 and σ_2) around crack α and discontinuity β with distance of $3a$ and $2a$ respectively. In these

examples, a tensile mean stress (positive value) is concentrated between the crack tip and end of discontinuity causes the rocks fail by cracking.

Due to stress concentration on the crack tips, crack starts to initiate from crack tips, which end up with crack interaction. Decreasing the distance between the crack and discontinuity increases the interaction effect and consequently interaction stresses. Therefore, stress concentration on the crack tip for the distance of $3a$ is smaller than that of the distance of $2a$. In the general form, the path of fracture will be changed with alteration in distance and inclination of discontinuity.

For this reason, crack propagation path for different inclination angles of inclined discontinuity in two distances is studied with MTS (σ - criterion) and SED (S-criterion) criteria. Figure 13 shows the paths of crack for distance $3a$. The results show that the crack propagation path for 90-degree inclined discontinuity is in straight line, but for 15-degree inclination the crack reorients and then interacts with discontinuity at right angle. Figure 14 shows the fracture propagation path deviates earlier with decreasing inclination angle of crack α . In addition, the angle of interaction reduces with crack α angle of inclination decreasing.

Figure 15 shows the paths of crack for distance 2a. the results show that the path for 90 degree inclined discontinuity is in straight form too, and with decreasing angle of discontinuity, the fracture propagation path deviates earlier. It is mentioned that all of crack propagation paths deviate earlier than distance 3a. These results have agreement with the results from tensional zones that show in the Figures 12 and 13. We can show that the results of σ -criterion is close to S-criterion for both distances 2a and 3a. This is related to brittle failure of rock ($\nu=0.2$) and large value of KI. In hydraulic fracture propagation, the pressure inside the fracture makes the value of KI be greater than the KII and then related to the figure 4 the propagation angle from S- criterion is closed

to the σ - criterion. The comparison of paths of cracks with distances 2a and 3a from discontinuity at a 15-degree angle is shown in figure 16 and the mean stress around the two equal cracks with distance 3a is presented in the figure 17.

7.2. Hydraulic fracturing and discontinuity with different inclination

A better understanding of how an induced fracture interacts with a discontinuity is fundamental for predicting the ultimate size and shape of the hydraulic fractures formed by a treatment. In this example, the effect of discontinuity on the path of hydraulic fracture is studied.

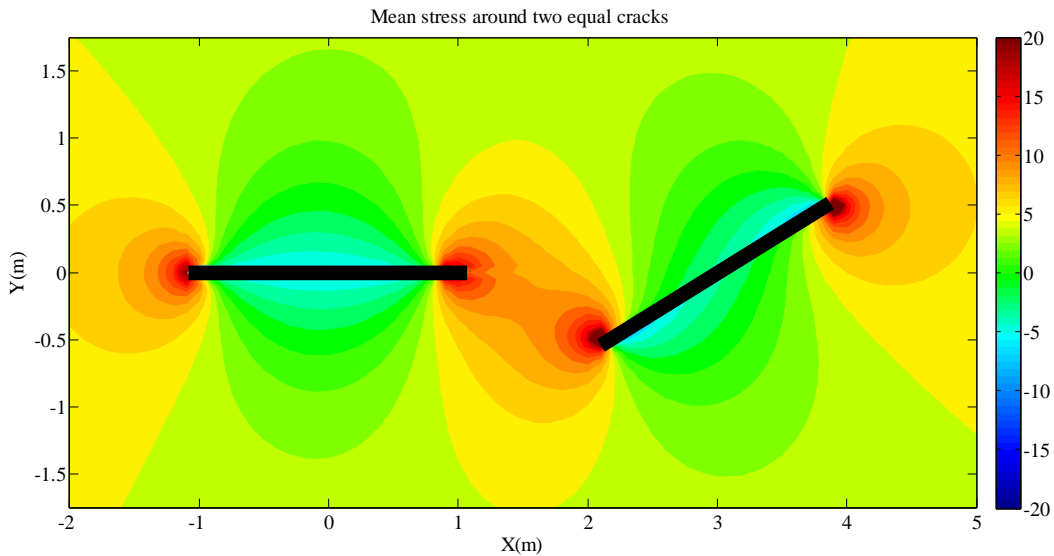


Figure 12. Mean stress around two equal cracks with ratio $c/a=1.5$. The inclination angle is 30 degree

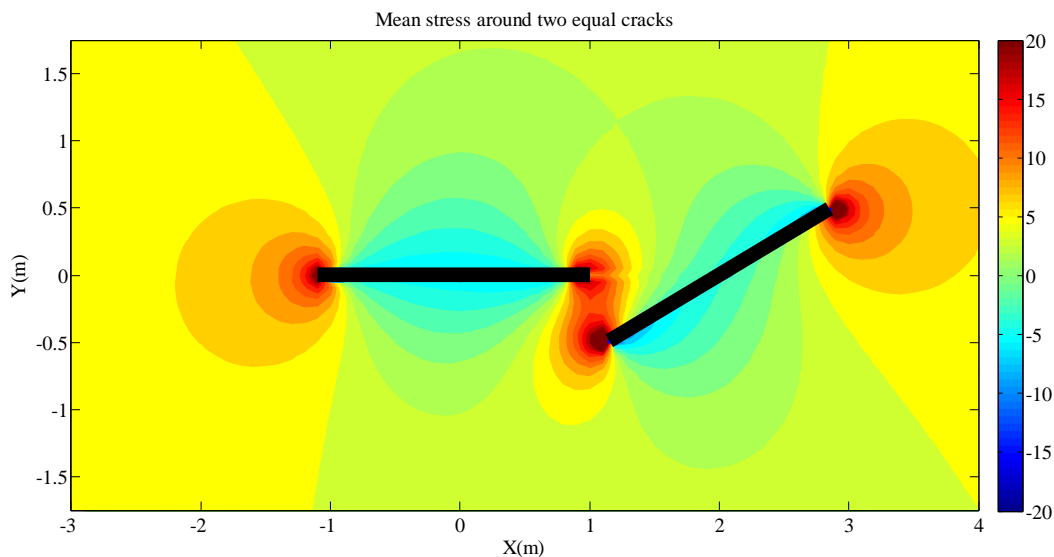


Figure 13. Mean stress around two equal cracks with ratio $c/a=1.0$. The inclination angle is 30 degree

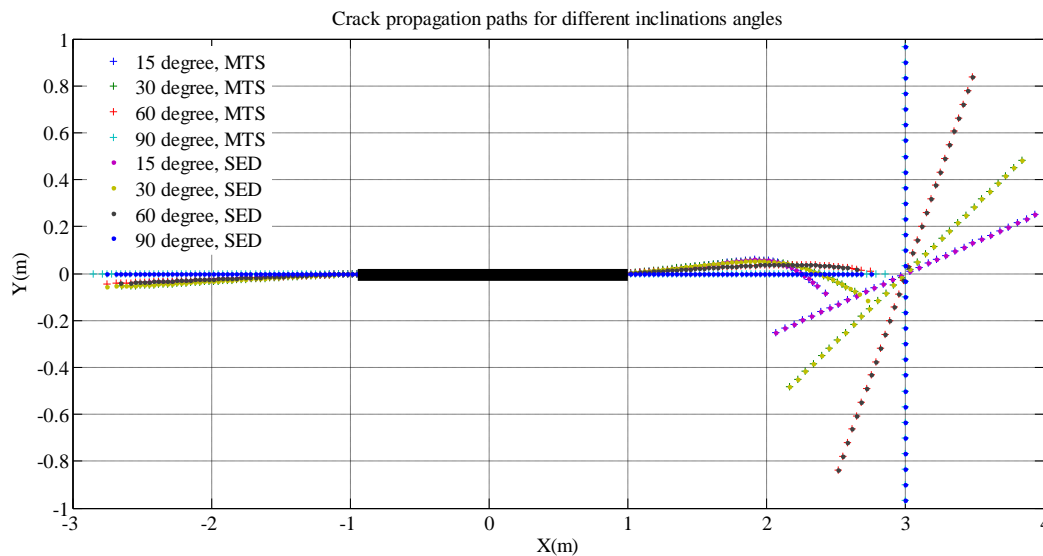


Figure 14. crack propagation path for different inclination angles of discontinuity with ratio $c/a=1.5$

The physical properties are $E=10$ GPa, $\nu = 0.25$, $KIC=2$ MPa $m^{0.5}$. The maximum compressive horizontal stress (X-axis) and minimum compressive horizontal stress (Y-axis) are 7 and 2 MPa respectively, and the pressure inside the fracture is 10 MPa. Figure 18 shows the paths of hydraulic fracturing for distance $2a$. The path of fracture when interacts with discontinuity with 90-degree inclination is in straight line, but with decreasing inclination angle the fracture deviates from its direction and reorients sooner. Discontinuity changes the field stress near its surface and causes the principal stresses to be locally parallel and perpendicular to the surface, therefore all fractures tend to interact with discontinuity at right angle. The paths from both criteria are near together, that is related to Poisson ratio and magnitude of KI and KII in the fracture tip.

7.3. Hydraulic fracturing and parallel discontinuities

Discontinuities that are parallel with pressurized fracture influence the propagation of fracture. This study considers the effect of spacing between the parallel discontinuity and pressurized crack in X and Y direction. The properties of material and stress condition are the same as those mentioned in section 7.2. The geometry and results are shown in figure 19 and 20. For the first example (Figure 19), the distance between the discontinuity and fracture is changed in X direction and the distances in Y direction are constant. The results show when the fracture propagates under discontinuity, the path of

fracture deviates towards the discontinuity and then propagates in its direction, but finally level of propagation will change and have a jump. This change in level of hydraulic fracture path is greater for discontinuity that is farther than the other discontinuity.

In the second example (Figure 20), the distance between the discontinuity and fracture is changed in Y direction and the distances in X direction will be constant. Results show with increasing the distance in Y direction the influence of discontinuity on propagation path will be less and fracture tend to propagate near its plane, but for the smallest spacing the mechanical interaction between the fracture and discontinuity is greatest and the path has the greatest curvature, therefore for different distances fracture propagates in different level.

8. Conclusion

This paper presents a numerical method for mixed-mode crack tip propagation of pressurized fractures in remotely compressed rocks. The maximum tangential stress criterion is implemented sequentially to trace the crack propagation path. Results derived from this numerical method are compared with those available in the literature showing that the results are accurate and in most cases error is less than one percent.

Stress intensity factors computed by the approximate method are very close to that obtained from analytical solution for the fracture mechanics problem studied in this paper. Crack tip propagation angles obtained from the proposed numerical method are compared with that

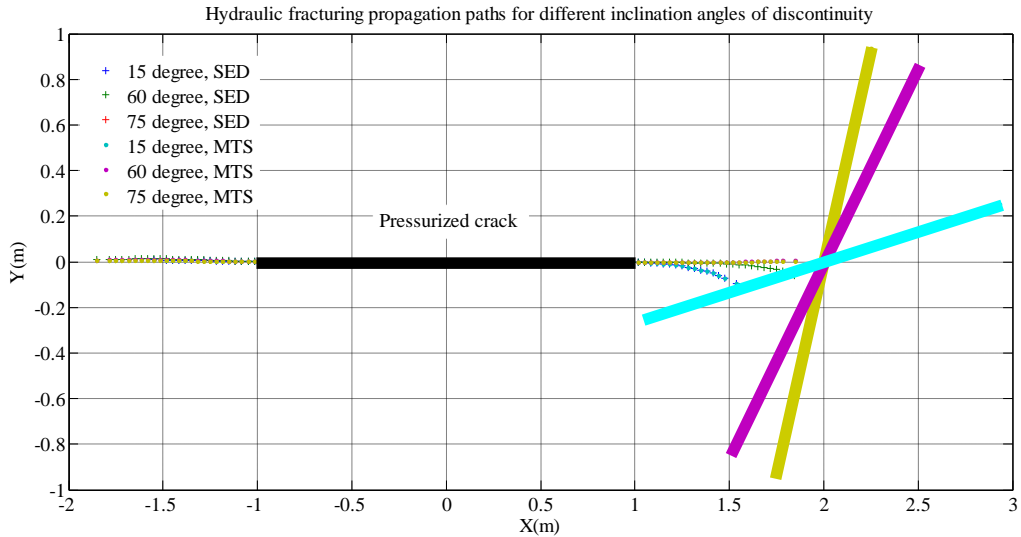


Figure 18. Hydraulic fracturing propagation paths for different inclination angles of discontinuity with distance $c/a=1$

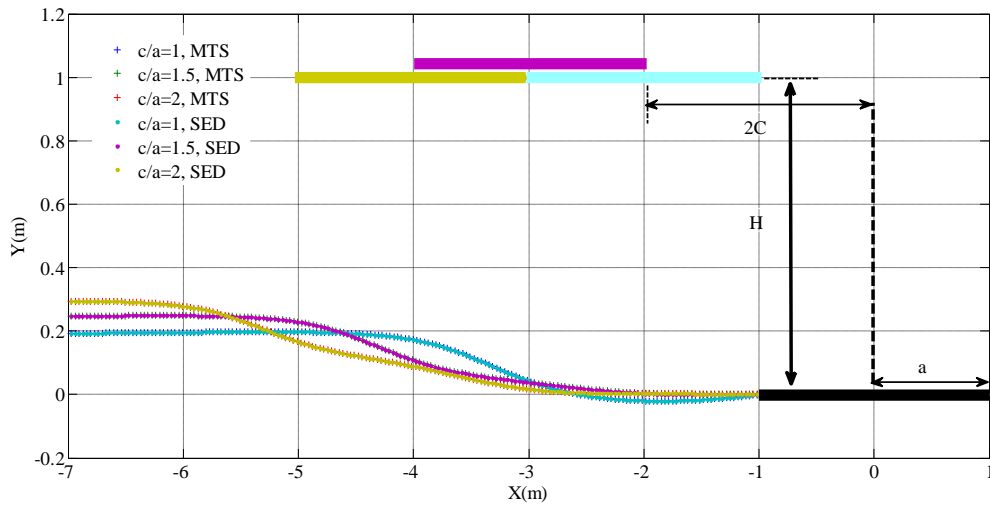


Figure 19. Paths of pressurized crack that is parallel to discontinuity for different distances in X Direction. $P=-10$ MPa, $\sigma_H=-7$ MPa, -2 MPa, and $H/a=1$

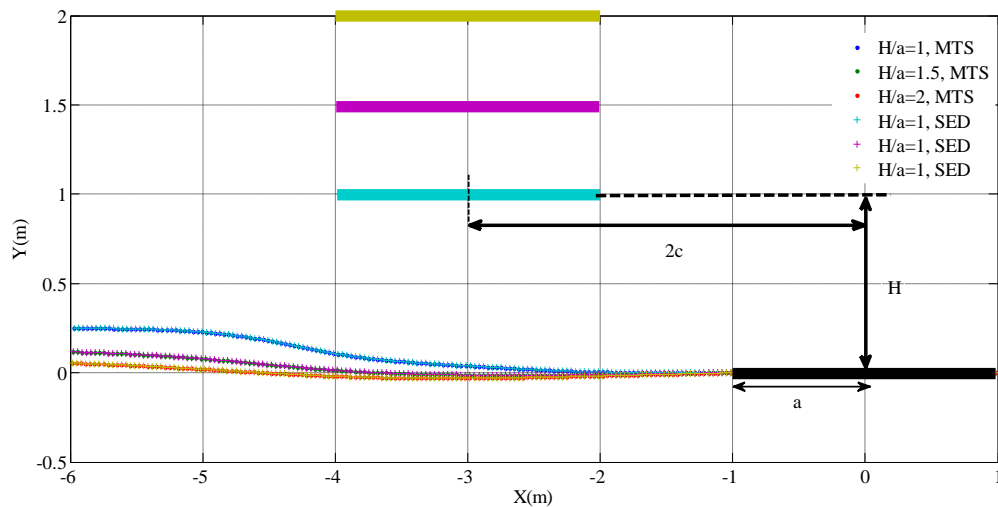


Figure 20. Paths of pressurized crack that is parallel to discontinuity for different distances in Y Direction. $P=-10$ MPa, $\sigma_H=-7$ MPa, -2 MPa, and $c/a=1.5$

available in the literature showing the high accuracy of the method.

The maximum tangential stress criterion and the minimum strain energy density give the same results under the brittle condition. Their results are very close to each other for propagation of hydraulic fracture near the discontinuities (it may be due to large value of K_{II} in hydraulic fracturing propagation and low value of Poisson ratio for brittle rocks). In general, at a small ratio of K_{II}/K_I , the two criteria show little difference, which can be noticed from figure 4. Fortunately, propagation of a hydraulic fracturing takes place in this region and the fracture path is the same for two criteria.

It was found that by increasing the discontinuity inclination angle, α , the angle of interaction also increases. For an inclination angle of 90 degree, the angle of interaction of hydraulic fracture reaches its maximum value (90 degree). Furthermore, by decreasing the discontinuity inclination angle, hydraulic fracturing propagation path deviates from its original route earlier. Regarding the spacing between the hydraulic fracture and discontinuity, the stress concentration on the crack tip is larger over the smaller distances due to the bigger interaction effect.

References

[1]. Clark, J. B., (1949). A hydraulic process for increasing the productivity of wells. Petroleum Transactions. American Institute of Mining and Energy., 186: 1-8.

[2]. Kachanov, L.M. (1986). Introduction to continuum damage mechanics, Martinus Nijhoff, Dordrecht.

[3]. Golshani, A., Yoshiaki, O., Masanobu, O. and Takemura, T. (2006). A micromechanical model for brittle failure of rock and its relation to crack growth observed in tri-axial compression tests of granite. Mechanics of Materials. 38 (4): 287-303.

[4]. Gross, D. and Seeling, T. (2006). Fracture mechanics: with an introduction to micromechanics, Springer.

[5]. Shen, B. and Stephansson, O. (1994). Modification of the G-criterion for crack propagation subjected to compression. Engineering Fracture Mechanics. 47(2): 177-189.

[6]. Vászárhelyi, B. and Bobet, A. (2000). Modeling of crack initiation, propagation and coalescence in uniaxial compression. Rock Mechanics and Rock Engineering. 33(2):119-139.

[7]. Dong C Y. and Pater C J. (2001). Numerical implementation of displacement discontinuity method and its application in hydraulic fracturing.,

Computational Methods in Applied Mechanics and Engineering. 191: 745-760

[8]. Aliabadi, M.H. and Rooke, D.P., (1991). Numerical fracture mechanics, Computational Mechanics Publications, Southampton, UK.

[9]. Aliabadi, M.H. (1998). Fracture of rocks, Computational Mechanics Publications, Southampton, UK.

[10]. Olson, J.E. and Pollard, D.D. (1988). Inferring stress states from detailed joint geometry. Proc: 29th US Symposium on Rock Mechanics, A.A. Balkema, Rotterdam, 159-167.

[11]. Olson, J.E. and Pollard, D.D. (1989). Inferring paleostresses from natural fracture patterns: A new method. Geology, 17: 345-348.

[12]. Olson, J.E. and Pollard, D.D. (1991). The initiation of en échelon veins. Journal of Structural Geology. 13(5): 595-608.

[13]. Chan, H.C.M., Li, V. and Einstein, H.H. (1990). A hybridized displacement discontinuity and indirect boundary element method to model fracture propagation. International Journal of Fracture. 45: 263-282.

[14]. Pollard, D.D., Zeller, S., Olson, J. and Thomas, A. (1990). Understanding the process of jointing in brittle rock masses. Proc: 31st US Symposium on Rock Mechanics, A.A. Balkema, Rotterdam, 447-454.

[15]. Zeller, S.S. and Pollard, D.D. (1992). Boundary conditions for rock fracture analysis using the boundary element method. Journal of Geophysical Research. 97(B2): 1991-1997.

[16]. Scavia, C. (1995). A method for the study of crack propagation in rock structures. Géotechnique. 45(3): 447-463.

[17]. Marji M. F. (1997). Modeling of cracks in rock fragmentation with a higher order displacement discontinuity method, PhD Thesis, Mining Engineering Department, Middle East Technical University, Ankara, Turkey.

[18]. Shou, K.J. and Crouch, S.L. (1995). A higher order displacement discontinuity method for analysis of crack problems. International Journal of Rock Mechanics and Mining Science and Geomechanics Abstract. 32: 49-55.

[19]. Tan, X.C., Kou, S.Q. and Lindqvist, P.A. (1996). Simulation of rock fragmentation by indenters using DDM and fracture mechanics. In: Aubertin, M., Hassani, F., Mitri, H. (Ed.), Rock Mechanics, Tools and Techniques. Balkema, Roterdam.

[20]. Marji M. F. and Hosseini Nasab, H. and Kohsary A. H. (2006). On the uses of special crack tip elements in numerical rock fracture mechanics International Journal of Solids and Structure., 43:1669-1692.

- [21]. Hossaini Nasab H. and Marji M. F. (2007). A semi-infinite higher-order displacement discontinuity method and its application to the quasistatic analysis of radial cracks produced by blasting., *Journal of Mechanics of Materials and Structures.*, 2(3).
- [22]. Marji M. F. and Dehghani I. (2010). Kinked crack analysis by a hybridized boundary element/boundary collocation method. *International Journal of Solids and Structures.*, 47 (7-8): 922-933.
- [23]. Bobet, A. and Einstein, H. H. (1998). Numerical modeling of fracture coalescence in rock materials. *International Journal of Fracture.*, 92: 221-252.
- [24]. Shen, B., Stephansson, O., Rinne, M., Lee, H.-S., Jing, L. and Roshoff, K. (2004). A fracture propagation code and its application to nuclear waste disposal. *International Journal of Rock Mechanics and Mining Science.* 41 (3): 448–453.
- [25]. Erdogan, F. and Sih, G.C. (1963). On the crack extension in plates under plane loading and transverse shear. *Journal of Basic Engineering.* 85: 519-527
- [26]. Hussain, M. A., Pu, S. L. and Underwood, J. (1974). Strain energy release rate for crack under combined mode I and mode II. *Fracture Analysis. ASTM STP 560: 2-28.*
- [27]. Sih, G.C. (1974). Strain-energy density factor applied to mixed mode crack problems. *International Journal of Fracture.* 10(3): 305–321.
- [28]. Ingraffea A. R. (1983). Numerical modeling of fracture propagation, In: *Rock Fracture Mechanics*, Rossmannith H. P. (Ed), Springer Verlagwien, New York, 151-208.
- [29]. Broek, D. (1989). *The Practical use of fracture mechanics*, fourth ed. Kluwer Academic Publishers, The Netherlands.
- [30]. Whittaker, B.N., Singh, R.N. and Sun, G. (1992). *Rock Fracture Mechanics, Principles, Design and Applications.* Elsevier, Netherlands.
- [31]. Ingraffea, A.R. (1981). Mixed-mode fracture initiation in Indiana Sandstone and Westerly Granite. In: Einstein, H.H. (Ed.), *Rock Mechanics from Research to Application. Proceedings of the 22nd US Symposium in Rock Mechanics.* MIT, Cambridge, MA, 199–204.
- [32]. Crouch, S.L. (1976). Solution of plane elasticity problems by the displacement discontinuity method. *International Journal for Numerical Methods in Engineering.* 10: 301–343.
- [33]. Crouch, S.L. and Starfield, A.M. (1983). *Boundary Element Methods in Solid Mechanics*, Allen and Unwin, London.
- [34]. Rossmannith, H. P. (1983). *Rock Fracture Mechanics*, Springer Verlagwien, New York.
- [35]. Ingraffea, A.R. (1987). Theory of crack initiation and propagation in rock. In: Atkinson, B.K. (Ed.), *Fracture Mechanics of Rock, Geology Series.* Academy Press, New York, pp. 71–110, pp. 151–208.
- [36]. Rao, Q., Sun, Z., Stephansson, O., Li, C. and Stillborg, B. (2003). Shear fracture (Mode II) of brittle rock. *International Journal of Rock Mechanics and Mining Science.* 40: 355–375.
- [37]. Guo, H., Aziz, N.I. and Schmidt, R.A. (1990). Linear elastic crack tip modeling by displacement discontinuity method. *Engineering Fracture Mechanics.* 36: 933–943.
- [38]. Scavia, C. (1992). A numerical technique for the analysis of cracks subjected to normal compressive stresses. *International Journal for Numerical Methods in Engineering.* 33: 929–942.
- [39]. Gdoutos, E.E. (1984). *Problems of mixed mode crack propagation*, Martinus Nijhoff, Dordrecht.
- [40]. Sih, G.C. (1973). *Methods of analysis and solutions of crack Problems. Mechanics of Fracture.*, vol. 1. Noordhoff. International Publishing, Leyden.
- [41]. Rice, J. R. (1968). *Mathematical analysis in the mechanics of fracture*, *Fracture: An Advanced Treatise.*, Vol. II, H. Liebowitz, Academic Press, New York, NY., 191-311.
- [42]. Cornet, F. H. (1982). Interpretation of hydraulic injection tests for in situ stress determination, *proc. Workshop on hydraulic fracturing stress measurements*, Haimson, B., Zobak, M.D., 149-158.
- [43]. Ching, H.Y. (1997). *Mechanics of hydraulic fracturing*, Gulf Publishing Company, Texas.